Effect of a magnetic field on the luminescent lifetime of Cu^+ in alkali halide host crystals

Stephen A. Payne*
Department of Chemistry, Princeton University, Princeton, New Jersey 08544

R. H. Austin
Department of Physics, Princeton University, Princeton, New Jersey 08544

Donald S. McClure
Department of Chemistry, Princeton University, Princeton, New Jersey 08544
(Received 15 August 1983)

We have measured the change in the triplet emission lifetime of the Cu^+ impurity in various alkali halide hosts at 4.2 K as a function of applied magnetic field. Pedrini [Phys. Status Solidi B 87, 273 (1978)] has proposed that the ^3E_g emitting state is split into T_{1g} and T_{2g} spin-orbit components and has found that the emission lifetime depends sensitively on the splitting. We have utilized an external magnetic field to mix these spin-orbit levels. This produced a measurable decrease in the emission lifetime which we explained with Pedrini's model. We also diagonalized the d^9s excited-state matrix to calculate independently the T_{1g},T_{2g} spin-orbit splitting and obtained reasonable agreement with our experimental results.

I. INTRODUCTION

The emission lifetime of the Cu^+ impurity in host crystals is observed to decrease strongly as the temperature rises from 4 K and to reach a nearly constant value around 77 K. Nonradiative quenching does not begin until much higher temperatures. Pedrini suggested that this behavior is due to the specific sublevel structure of the emitting triplet state and supported this hypothesis with an analysis of the kinetics of the emission process as a function of temperature.[1] We wanted to test Pedrini's hypothesis in a manner that does not require changing the temperature: As we will show below, a magnetic field should cause a mixing of the triplet sublevels, which Pedrini postulated. This mixing should cause a change of emission lifetime from which the level structure could be deduced. Therefore, we have measured the emission lifetime at 4 K as a function of magnetic field for five Cu^+-doped alkali halide crystals. A similar set of experiments done by Kabler, Marrone, and Fowler[2] helped to clarify the level structure of self-trapped excitons in alkali halides.

The Cu^+ ion has now been studied as a substitutional impurity in most of the alkali halide host crystals.[3] The ground state is d^{10}, and therefore no d-d transitions are observed; the first excited state is derived from the d^9s configuration. The energy levels of NaF:Cu^+ are quantitatively sketched in Fig. 1.[4,5] The free-ion levels are indicated on the far left.[6] The general increase in energy from free ion to crystal is due to the antibonding interaction of the Cu^+ 4s orbital with the fluorines.[7] The octahedral field splits the ^1D and ^3D into E_g and T_{2g} components. The further splitting of the E_g states shown on the diagram represents the Jahn-Teller energy. Lastly, the T_{1g} and T_{2g} spin-orbit (SO) components expected to arise from a ^3E_g state are indicated. The orbital angular momentum of an E_g state is quenched, and therefore the spin-orbit splitting arises from the interaction of the ^3E_g with the $^1T_{2g}$ and $^3T_{2g}$ states. (Since all symmetries are gerade in this paper, we now drop the g subscripts.)

Following the absorption of a photon by the $^1A_1 \rightarrow {}^1E$ or $^1A_1 \rightarrow {}^1T_2$ transition, the energy settles to the lowest SO components of ^3E designated as $T_1(^3E)$ and $T_2(^3E)$, and thermal equilibrium is rapidly achieved. Since the $T_2(^3E)$ mixes with the $^1T_2$ state by way of the SO interaction, it acquires significant singlet character ($\sim 1\%$) and the spin selection rules with the ground state are relaxed. The $T_1(^3E)$ level, however, cannot interact with the singlets in the d^9s manifold and thus obtains a much smaller amount of singlet character by higher-order mixings (e.g., with the

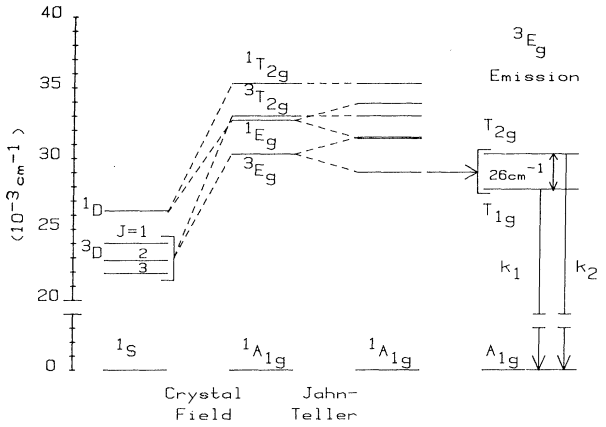

FIG. 1. Explanation of Cu^+ energy levels in alkali halide hosts (NaF). Left, free-ion levels; middle, effects of crystal-field and Jahn-Teller distortion, spin-orbit splitting not shown; right, spin-orbit splitting of lowest level (emitting states) on a different scale.

d^9p states). Hence the emission rate from the $T_2(^3E)$ level, k_2, is much greater than that of the $T_1(^3E)$ level, k_1; see Fig. 1. Pedrini[1] first observed and explained this effect by studying the temperature dependence of the emission lifetime. As one might expect, the lifetime is long at $T<30$ K (emission mostly from T_1), and plateaus to a smaller value at $T>200$ K (emissions both from T_1 and T_2). Since the Cu^+ emission do not quench until temperatures greater than 500 K are achieved,[8] radiationless processes do not affect the observed lifetimes.

It is possible to mix the T_1 and T_2 levels by means of an external magnetic field. The Zeeman operator belongs to the T_2 representation, and therefore the matrix elements $\langle T_1 \mid \vec{H}\cdot(\vec{L}+2\vec{S}) \mid T_2 \rangle$ need not be zero. This mixing would cause an increase in the emission rate at 4.2 K since more singlet would be mixed into T_1 via the T_2 level; recall that T_1 alone is populated at 4.2 K (refer to Fig. 1). We expect this mixing to be on the order of $(\mu_B H/\Delta)^2$, where μ_B is the Bohr magneton, H is the magnetic field, and Δ is the T_1,T_2 splitting (or "zero-field splitting"). Using typical values of $H=40$ kG and $\Delta\sim 50$ cm^{-1}, we get $(\mu_B H/\Delta)^2=0.001$. Taking $k_2/k_1\sim 100$, we expect the 4.2 K emission rate to increase by $(0.001)(k_2/k_1)\sim 10\%$. Changes of this amount can be measured by modern methods of transient digitization and computerization.

In Sec. II the experimental method is described. In Sec. III we outline the theory of the magnetic effect. The results are shown in Sec. IV, where they are fit to the theory we have developed. In Sec. V we explain the trends of the T_1,T_2 splitting observed in the five Cu^+-doped crystals studied: LiCl, NaCl, KCl, NaF, and NaBr.

II. EXPERIMENTAL

The apparatus we used is similar to that of Ref. 9. The exciting source was a frequency-quadrupled, Nd:yttrium aluminum garnet (YAG) pulsed laser (Molectron Model MY-32), operating at 10 Hz. The laser wavelength of 265 nm fortunately coincides with the uv absorption of the Cu^+ impurity in all the crystal hosts studied. The sample was immersed in helium in the Oxford Instruments cryostat-superconducting magnet system, Spectro-Mag IV, used in Ref. 10. The resulting blue or uv emission from the sample was isolated with appropriate Corning filters and detected by an EMI 6285B photomultiplier tube (PMT). The PMT response was amplified and then sent to a Biomation 6500 transient recorder. The average of 512 curves was sent to a microcomputer and stored. The emission decays were later fit to one or two exponential functions of time, as required.

All the samples except for NaBr were large (3–10 mm)^3 single crystals. These samples were oriented so $\vec{H}\|[100]$. The NaBr sample was a small crystallite and was not oriented. Nevertheless, the theory of the next section is still applicable. The crystals were thermally quenched from 400°C to room temperature to remove Cu^+-aggregate absorptions.

III. THEORY

Since the $T_2(^3E)$ level is much closer to the T_1 level than to any other level, we formulate the problem solely in terms of this interaction. The Hamiltonian can be written as

$$\mathcal{H}=\mathcal{H}_0+\mathcal{H}_{\text{Zeeman}}\,, \tag{1}$$

where

$$\mathcal{H}_{\text{Zeeman}}=\frac{\mu_B}{\hbar}(\vec{L}_z+2\vec{S}_z)\cdot\vec{H}_z \tag{2}$$

if we take z as the field direction, [100]. From Griffith's tables[11] we decompose the SO state into the spin s and orbit o parts:

$$|\,\Gamma\gamma\rangle=\sum_{\substack{e=\theta,\epsilon\\ t=-1,0,+1}}\langle E,e,T_1,t\,|\,\Gamma\gamma\rangle\,|\,E,e\rangle_0\,|\,T_1,t\rangle_s\,, \tag{3}$$

where $\Gamma\gamma$ is a component of T_1 and T_2. Within the d-orbital approximation, we write

$$|\,E,\theta\rangle=|\,2,0\rangle$$

and

$$|\,E,\epsilon\rangle=\frac{1}{\sqrt{2}}(\,|\,2,2\rangle+|\,2,-2\rangle)\,. \tag{4}$$

We also know that

$$|\,T_1,1\rangle_s=|\,1,1\rangle\,,\quad |\,T_1,0\rangle_s=|\,1,0\rangle\,,$$

and

$$|\,T_1,-1\rangle_s=|\,1,-1\rangle\,. \tag{5}$$

Using Eqs. (3)–(5), we formulate the Zeeman matrix of $S_z/\hbar$ as

	$\lvert T_1,1\rangle$	$\lvert T_2,-1\rangle$	$\lvert T_1,-1\rangle$	$\lvert T_2,1\rangle$
$\langle T_1,1\rvert$	$-\frac{1}{2}$	$-\frac{\sqrt{3}}{2}$	0	0
$\langle T_2,-1\rvert$	$-\frac{\sqrt{3}}{2}$	$\frac{1}{2}$	0	0
$\langle T_1,-1\rvert$	0	0	$\frac{1}{2}$	$\frac{\sqrt{3}}{2}$
$\langle T_2,-1\rvert$	0	0	$\frac{\sqrt{3}}{2}$	$-\frac{1}{2}$

(6)

The L_z operator in Eq. (2) is not important since the orbital angular momentum is quenched for an E state, and therefore we take the g factor as 2. Since there is no spin-orbit coupling within the ^3E state, we can neglect the influence of the Jahn-Teller distortion on the value of Δ. Using Eq. (2) and setting $\mu_B H=F$, we find the resulting T_1 wave functions expressed in terms of the zero-field states are

$$\begin{aligned}
|\,T_1,+1\rangle_F&=|\,T_1,+1\rangle_0+\frac{\sqrt{3}F}{(\Delta^2+4\Delta F)^{1/2}}\,|\,T_2,-1\rangle_0\,,\\
|\,T_1,0\rangle_F&=|\,T_1,0\rangle_0\,,\\
|\,T_1,-1\rangle_F&=|\,T_1,-1\rangle_0-\frac{\sqrt{3}F}{(\Delta^2-4\Delta F)^{1/2}}\,|\,T_2,+1\rangle_0\,,
\end{aligned} \tag{7}$$

and their energies are

$$E(T_1,+1)=-F,\quad E(T_1,0)=0$$

and

$$E(T_1,-1)=+F\,. \tag{8}$$

We have obtained these results by neglecting terms of the order $(F/\Delta)^2$ and by using Taylor-series expansions at the appropriate opportunities.

The spontaneous radiation rates from the T_2 and T_1 states at zero field at an average wavelength λ are as follows:

$$k_2=k_{T_2(0,\pm1)}=\frac{64\pi^4}{3h\lambda^3}\,|\langle A_1,a\,|\,O_p\,|\,T_2,(0\pm1)\rangle|^2 \tag{9}$$

and

$$k_1=k_{T_1(0\pm1)}=\frac{64\pi^4}{3h\lambda^3}\,|\langle A_1,a\,|\,O_p\,|\,T_1,(0\pm1)\rangle|^2\,, \tag{10}$$

where O_p is the photon operator by which the transition occurs. Taking the Boltzmann thermal population of the T_1 sublevels into account, we find that the observed rate of emission for the wave functions of Eqs. (7) is

$$k_F=\frac{\left[\exp\left[\frac{F}{kT}\right]\left[k_1+\frac{3F^2}{\Delta^2+4\Delta F}k_2\right]+k_1+\exp\left[\frac{-F}{kT}\right]\left[k_1+\frac{3F^2}{\Delta^2-4\Delta F}k_2\right]\right]}{\left[\exp\left[\frac{+F}{kT}\right]+1+\exp\left[\frac{-F}{kT}\right]\right]}\,. \tag{11}$$

k_1 and k_2 represent the zero-field emission rate of the T_1 and T_2 states at 4.2 K. Since T_1 is exclusively populated at 4.2 K, k_1 is simply the inverse of the observed zero-field lifetime. k_2, on the other hand, cannot be observed at 4.2 K. At 300 K, the population is almost equally divided between T_1 and T_2. Since $k_1 \ll k_2$, the 300-K emission rate multiplied by 2 represents the T_2 rate at 300 K, $k_2(300\text{ K})$. The emission rate from T_2 may depend on temperature for the same reasons as does the absorption, namely, the $g\rightarrow g$ transition can only become allowed through static or dynamic displacements which destroy the center of symmetry. Whether static (temperature independent) or dynamic (temperature dependent) or a mixture of these perturbations destroy the symmetry cannot be known until numerous details of the potential function for Cu^+ in the triplet state are known. Therefore, we make the simplest approximation by assuming that the T_2 emission rate is independent of temperature, i.e., $k_2(300\text{ K})=k_2(4.2\text{ K})$. After obtaining k_1 and k_2 from the low- and high-temperature emission rates, we fit the magnetic field dependence to Eq. (11) in order to determine the zero-field T_1,T_2 splitting Δ. We can compare our values of Δ to the values calculated by Pedrini from the temperature dependence of the emission lifetime.

IV. RESULTS

Figures 2 and 3 show the emission rate plotted against the magnetic field. In passing we note that LiCl and NaCl have short lifetimes of 70 and 56 μs in addition to the much longer lifetimes which are plotted in Figs. 2 and 3. Since these lifetimes could not be evaluated as precisely, their field dependence could not be determined. NaF, on the other hand, was accurately fit to a single exponential. Excessive scattering from the NaBr sample precluded short time measurement. KCl, however, presented special problems because it was deconvolated into a double exponential with two similar lifetimes of approximately 136- and 435-μs duration. The least-squares analysis was

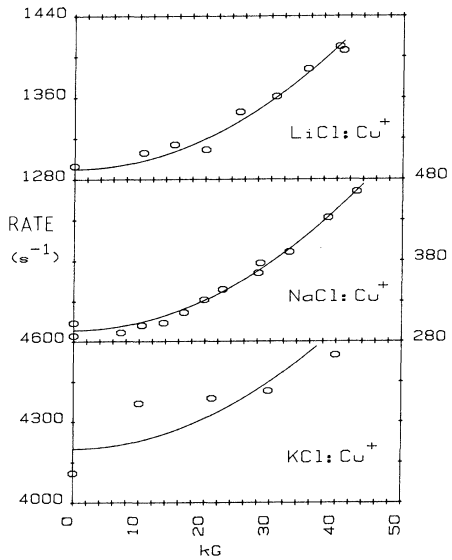

FIG. 2. Dependence of ^3E emission rate on magnetic field strength for Cu^+ in LiCl, NaCl, and KCl at 4.2 K.

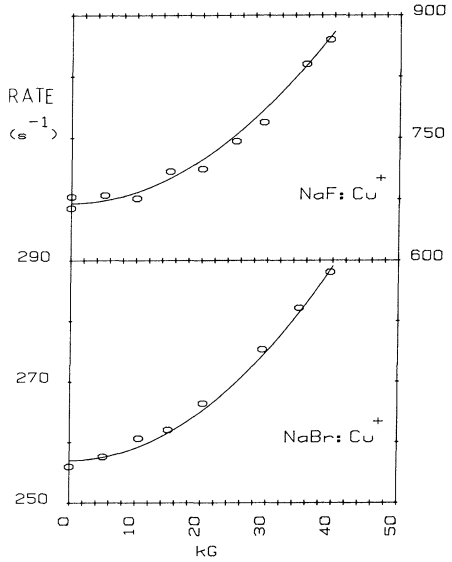

FIG. 3. Dependence of ^3E emission rate on magnetic field strength for Cu^+ in NaF and NaBr at 4.2 K.

TABLE I. T_2 emission rate k_2 and T_1 emission rate k_1 are listed; T_1,T_2 zero-field splitting Δ determined by this work and from the literature is shown.

Crystal	k_2 (s^{-1}) (Ref. indicated)	k_1 (s^{-1}) (This work)	Δ (cm^{-1}) (This work)	Δ (cm^{-1}) (Ref. indicated)
LiCl[a]	61 700	1290	60	80
NaCl[b]	45 900	294	46	36
KCl[c]	80 100	4200	35	18
NaF[d]	21 100	670	26	31
NaBr	16 600	257	60	

[a] Reference 1.
[b] Reference 12.
[c] Reference 14.
[d] Reference 13.

somewhat uncertain, since the quality of the fit did not vary much with changes in the two lifetimes. To reduce this error the geometric mean of the two rates is reported in Fig. 2.

It is apparent that the emission rate increases with field in all cases shown in Figs. 2 and 3, as predicted. In fitting the data to Eq. (11), we use $k_1=1/\tau(4.2\text{ K})$ and $k_2=2/\tau(300\text{ K})$, as previously discussed. The relevant parameters are shown in Table I.[1,12–14] It is seen that our determinations of Δ agree well with those of Pedrini [LiCl,[1] NaCl,[12] NaF (Ref. 13)]. The poor agreement with KCl is, in part, due to the scatter of our data. We obtained the value $\Delta=18$ cm^{-1} from Ref. 14 by analyzing their data with Pedrini's formula.[1] Since they have not recognized the dual exponential nature of KCl:Cu^+ triplet emission, the validity of their number is also in question.

For given values of k_1 and k_2, the random errors in k_F give Δ within a few inverse centimeters. The value of k_1 is known to within a few percent. The choice of k_2, therefore, has the greater effect on the value of Δ calculated from k_F through Eq. (11). The assumption that k_2 is measured by $k_F(300\text{ K})$ is the main source of uncertainty in the value of Δ. For example, in the case of LiCl, if we used $k_2=31\,000$ rather than $62\,000$ s^{-1}, the value of Δ would be 42 cm^{-1} rather than 60 cm^{-1}. Our choice of k_2 was the easiest to apply and gave reasonable agreement with Pedrini's values.[1,12,13]

V. DISCUSSION

The T_1,T_2 splitting can be studied by diagonalizing the matrix that describes the d^9s configuration. The d^9s SO matrix has been evaluated by Chermette and Pedrini[15] and is easily extended to include the crystal-field splitting and the exchange interaction by adding $10Dq$ to the diagonal matrix elements of the $^1T_2$ and $^3T_2$ states and G_2 to those of the ^1E and $^1T_2$ states, respectively.[16] The SO parameters ζ' and ζ are defined in the notation of Sugano *et al.*[17] as

$$\zeta'=\frac{i}{3\sqrt{2}}\langle t_2||v(1T_1)||e\rangle \tag{12a}$$

and

$$\zeta=\frac{-i}{3}\langle t_2||v(1T_1)||t_2\rangle\ , \tag{12b}$$

where the reduced matrix elements entail the t_2 and e one-electron orbitals and the SO operator. In the d-function approximation $\zeta=\zeta'$. If we use the free-ion values of $G_2=3630$ and $\zeta'=\zeta=-828$ cm^{-1} and plot Δ against $10Dq$, the middle curve in Fig. 4 is obtained. We note that Δ is about 80 cm^{-1} at a typical value of $10Dq=3000$ cm^{-1}. This is close to the experimental splittings listed in Table I. Thus a simple theory of the d^9s configuration has provided a value of Δ in reasonable agreement with experiment.

This calculation scheme also produces a good estimate of the emission lifetime at 300 K, as follows. First we use the formula

$$f_t=\frac{1.5}{\nu^2\tau_t} \tag{13}$$

to relate the lifetime of the ^3E state, τ_t (in s), to its oscillator strength f_t and the emission band energy ν (in cm^{-1}). In addition, the singlet, triplet oscillator strengths can be related by

$$f_t=|C_s|^2 f_s\ , \tag{14}$$

where C_s determines the amount of singlet mixed into

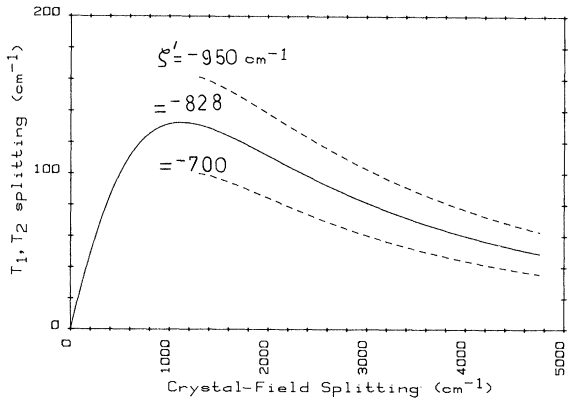

FIG. 4. Calculation of T_1,T_2 zero-field splitting as a function of the crystal-field parameter $10Dq$ for three values of the spin-orbit coupling parameter ζ' as indicated; free-ion values of exchange splitting $G_2=3630$ cm^{-1}, and SO coupling $\zeta=-828$ cm^{-1}, are used; T_1 and T_2 SO states are both correlated to the free-ion $^3D_3$ state at $10Dq=0$ for $\zeta=\zeta'$ (solid curve).

the $T_2(^3E)$ state, $|T_2(^3E)\rangle = C_s|^1T_2\rangle + C_{t1}|^3E\rangle + C_{t2}|^3T_2\rangle$. For LiCl:$Cu^+$, $f_s = 0.01$ and $\bar{\nu} = 31\,000$ cm^{-1} at 300 K.[1,7] Our d^9s matrix calculation shows that C_s remains relatively constant at 0.10 for any reasonable choice of input parameters. Using Eqs. (13) and (14), we get $1/\tau = 64\,000$ s^{-1}. This agrees well with the value of k_2 in Table I. Thus the value of C_s given by the theory is an accurate one.

From Table I we see that the T_1, T_2 splitting obtained for LiCl, NaCl, and KCl is 60, 46, and 35 cm^{-1}, respectively. Thus the value of Δ decreases with increasing cation size. Since the crystal-field splitting increases with smaller lattice constant, Fig. 4 suggests that Δ should be largest for KCl. This is contrary to experimental observation. There are several factors neglected in this calculation: covalency, Jahn-Teller distortion, and possible off-center distortions. The T_1, T_2 splitting depends sensitively on these and other factors, and we have not gone into a detailed study of them.

Δ is observed to increase with the atomic number of the halogen; for NaF, NaCl, and NaBr we have derived Δ as 26, 46, and 60 cm^{-1}. This increase may be related to the heavy-atom effect. To calculate it we must allow for the effects of covalency on the SO parameters. In the simplest approximation we assume that the e orbital will mix with the ligand p orbitals but the t_2 orbitals will remain pure:

$$\zeta = \zeta_d \tag{15a}$$

and

$$\zeta' = a\zeta_d - b\zeta_{Lp}\ , \tag{15b}$$

where ζ_d is the SO coupling constant of a d hole, and ζ_{Lp} is the one-electron SO coupling constant of the halogen. Since we cannot determine the constants a and b without detailed wave functions, we simply calculate two more curves in Fig. 4 with the free-ion values of G_2 and ζ, but now with ζ' at 950 and 700 cm^{-1} to represent the heavy-atom effect (Br^-) and orbital reduction (F^-), respectively. In agreement, the T_1, T_2 splitting does increase with a larger SO coupling constant, or physically, a heavier ligand, as experimentally determined (see upper and lower curves of Fig. 4). Nevertheless, this interpretation may have to be modified when a more rigorous theory of the ion in a crystal is carried out.

In conclusion, we have presented direct evidence that the temporal characteristics of the Cu^+ impurity emission are determined by the T_1 and T_2 SO levels of the ^3E state. The Pedrini two-state theory of emission was originally formulated from careful analysis of the temperature dependence of the emission lifetime. We believe that our magnetic experiments have provided important confirmation of Pedrini's theory.

The best determination of Δ would be by way of a direct spectroscopic method. The uv absorption into the triplet components will probably not be possible except perhaps for NaF:Cu^+, but the far ir absorption in the excited state may be possible.

ACKNOWLEDGMENTS

We wish to thank Professor Harry Drickamer for the NaBr:Cu^+ crystal and Professor Fritz Luty for the KCl:Cu^+ sample. We gratefully acknowledge many stimulating conversations with Dr. Christian Pedrini. This work was supported by the National Science Foundation, Grant No. CHE-82-10889.

*Present address: Department of Chemistry, University of Pennsylvania, Philadelphia, PA 19104.

[1] C. Pedrini, Phys. Status Solidi B 87, 273 (1978).
[2] M. N. Kabler, M. J. Marrone, and W. B. Fowler, in *Luminescence of Crystals, Molecules and Solutions,* edited by F. Williams (Plenum, New York, 1973), p. 171; W. B. Fowler, M. J. Marrone, and M. N. Kabler, Phys. Rev. B 8, 5909 (1973).
[3] M. Bertolaccini, P. Gagliardelli, G. Padovini, and G. Spinolo, J. Luminesc. 14, 281 (1976).
[4] S. A. Payne, A. B. Goldberg, and D. S. McClure, J. Chem. Phys. 78, 3688 (1983).
[5] A. B. Goldberg, D. S. McClure, and C. Pedrini, Chem. Phys. Lett. 87, 508 (1982).
[6] C. E. Moore, in *Atomic Energy Levels,* Natl. Bur. Stand. (U.S.) Circular (No. 467, U.S. G.P.O., Washington, D.C., 1949).
[7] J. Simonetti and D. S. McClure, Phys. Rev. B 16, 3887 (1977).
[8] R. Oggioni and P. Scaramelli, Phys. Status Solidi 9, 411 (1965).
[9] M. Hogan, J. Wang, R. H. Austin, C. L. Monitto, and S. Hershkowitz, Proc. Natl. Acad. Sci. USA 79, 3518 (1982).
[10] R. A. Shatwell and D. S. McClure, J. Chem. Phys. 70, 2081 (1979).
[11] J. S. Griffith, *The Theory of Transition Metal Ions* (Cambridge University Press, Cambridge, 1971).
[12] C. Pedrini and B. Jacquier, J. Phys. C 13, 4791 (1980).
[13] C. Pedrini (unpublished).
[14] M. Piccirilli and G. Spinolo, Phys. Rev. B 4, 1339 (1971).
[15] H. Chermette and C. Pedrini, J. Chem. Phys. 75, 1869 (1981).
[16] T. Yamaguchi (private communication).
[17] S. Sugano, Y. Tanabe, and H. Kamimura, *Multiplets of Transition-Metal Ions in Crystals* (Academic, New York, 1970).